Lattice Boltzmann equation hydrodynamics

I. Halliday, L. A. Hammond, C. M. Care, K. Good, and A. Stevens*
Materials Research Institute, Sheffield Hallam University, Pond Street, Sheffield S1 1WB, United Kingdom
(Received 16 October 2000; revised manuscript received 2 January 2001; published 28 June 2001)

By inserting position and time dependent ''source'' or ''forcing'' terms into the microscopic evolution equation of a lattice Boltzmann fluid and treating the generalized scheme within the usual Chapman-Enskog methodology, we show that the emergent dynamics of the lattice fluid may be usefully transformed. Our method of adjustment is demonstrated by implementing the cylindrical polar coordinate form of the continuity and momentum equations on a rectangular lattice and generating results for pipe flow. With straightforward systematic adjustment of the simulation, our approach produces results in excellent agreement with theory.

DOI: 10.1103/PhysRevE.64.011208 PACS number(s): 47.11.+j, 47.60.+i, 47.15.−x

I. INTRODUCTION

It was the work of Frisch *et al.* [1] on lattice gas automata that first suggested a lattice Boltzmann (LB) equation approach to hydrodynamics. Essentially LB calculations evolve a lattice-based momentum distribution function $f_i(\mathbf{r},t)$ and calculate the emergent lattice fluid's momentum $\rho\mathbf{v}$ and density ρ from this distribution and its moments with the lattice basis $\mathbf{c}_i$. As a model of the Boltzmann equation [2] and (after a number of crucial innovations [3–8]) as a complement to traditional methods of flow computation, the LB method continues to attract the interest of a growing international community.

Of the various LB approaches to flow computation the eponymous lattice Bhatnagar-Gross-Krook (LBGK) [9] scheme is the simplest. Indeed it contains only a scalar relaxation parameter $1/\tau$ and an *equilibrium* momentum distribution function $f_i^{(0)}(\rho,\mathbf{v})$ by which the macrodynamics of the lattice fluid may be determined—that is, made to conform with the incompressible Navier-Stokes and continuity equations. Reference [14] provides a particularly useful account of this analysis).

It is the aim of the present work to demonstrate how the form of the macroscopic equations describing the lattice fluid can be usefully adjusted by adding variable source terms to the microscopic evolution equation of the momentum densities—Eq. (7) below. Our aim is not, from a fundamental standpoint, to incorporate the effects of an external force upon the lattice fluid; rather, we aim to introduce extra terms self-consistently in the lattice fluid's momentum equation, in our case terms characteristic of, for example, a different geometry. For the sake of definiteness, we consider in the present work, a forcing strategy to recover, as the macroscopic equations of the lattice fluid, the cylindrical polar coordinate form of the Navier-Stokes and continuity equations. In Sec. II, an appropriate form of these equations is set out. In Sec. III we present a general analysis of forcing, which proceeds then to focus on the particular problem of Sec. II. In Sec. IV we detail the implementation of a test bench for the scheme devised in Sec. III and present results. Conclusions are presented in Sec. V.

II. REPRESENTING FLOW IN A CIRCULAR CHANNEL

We consider the problem of the laminar flow of an incompressible, isotropic liquid in internal flow with rotational symmetry around the z axis. Accordingly, the azimuthal velocity v_ϕ and ϕ coordinate derivatives vanish from the incompressible Navier-Stokes and continuity equations [11]. The remaining radial and axial velocities v_r and v_z and pressure P satisfy three equations in the two spatial coordinates z and r. On making the replacements

$$\begin{aligned}(z,r)&\rightarrow(x,y),\\ (v_z,v_r)&\rightarrow(v_x,v_y),\end{aligned} \tag{1}$$

we obtain a pseudo-Cartesian representation:

$$\partial_x v_x+\partial_y v_y=-\frac{v_y}{y}, \tag{2}$$

$$\frac{Dv_x}{Dt}=-\frac{1}{\rho}\partial_x P+\nu\nabla^2 v_x+\nu\frac{1}{y}\partial_y v_x, \tag{3}$$

$$\frac{Dv_y}{Dt}=-\frac{1}{\rho}\partial_y P+\nu\nabla^2 v_y+\nu\frac{1}{y}\left(\partial_y v_y-\frac{v_y}{y}\right). \tag{4}$$

The last terms on the right hand sides of Eqs. (2)–(4) we henceforward designate ''nonrectangular.''

We shall show that Eqs. (2)–(4) may be obtained from a lattice Boltzmann scheme simulating incompressible flow, with the following macroscopic equations for the two unknown quantities v_x and v_y:

$$\partial_t\rho+\partial_x\rho v_x+\partial_y\rho v_y=-\frac{1}{y}\rho v_y, \tag{5}$$

$$\frac{D\rho v_\alpha}{Dt}+\partial_\alpha P-\nu\nabla^2\rho v_\alpha=\frac{\nu}{y}\partial_y\rho v_\alpha-\frac{\nu\rho v_y}{y^2}\delta_{\alpha y}, \tag{6}$$

where $\alpha=x,y$.

[1]*Present address: Rolls-Royce, P.O. Box 2000, Derby, DE21 7XX, U.K.

The right-hand side (RHS) terms in continuity and momentum equations (5) and (6) arise from the particular way in which our simulation has been adapted to cylindrical polar coordinates, and not from external, physical accelerations impressed upon the fluid. It should be noted, however, that any such momentum equation acceleration (body force) terms could be treated phenomenologically with the approach we discuss in the next section. But, in a manner consistent with the analysis of Ref. [2] extended to apply to the Boltzmann equation with an acceleration term, Luo has shown how external, conservative body forces can emerge from an LB scheme [12]. We shall return to this issue in Sec. III D.

III. FORCING FLOW IN A LATTICE BOLTZMANN SIMULATION

A. General considerations

In the present work we seek to obtain the macrodynamics in Eqs. (5) and (6) from a two-dimensional, nine-velocity (2D9Q) lattice Bhatnagar-Gross-Krook fluid [13], which we shall modify. Note, however, that our analysis would generalize directly to any particular LB scheme.

For convenience we employ common lattice Boltzmann notation and for brevity construct our analysis around the formalism of Hou *et al.* [14], for their analysis of Qian, d'Humières, and Lallemand's LBGK algorithm [13] and the Chapman-Enskog expansion in particular, provides an appropriate basis for present work.

With the intention of driving the lattice fluid toward a nonuniform momentum distribution we incorporate a *spatial and velocity dependent* microscopic term $h_i(\mathbf{r},t)$ into an adjusted evolution equation for the lattice fluid's momentum distribution:

$$f_i(\mathbf{r}+\mathbf{c}_i\delta_t,t+\delta_t)=f_i(\mathbf{r},t)+\frac{1}{\tau}[f_i^{(0)}(\mathbf{v},\rho)-f(\mathbf{r},t)]+h_i(\mathbf{r},t) \tag{7}$$

where δ_t is the explicit time step and all other terms have their usual meaning [14]. For purposes of extracting the dynamics of this modified scheme (7) we perform a Chapman-Enskog type expansion with the h_i, like the f_i, expanded in powers of δ_t. Bearing in mind that, in the corresponding unadjusted LBGK scheme [13], the $\delta_t^n f_i^{(n)}$, $n>0$, model *departures* from equilibrium, we therefore take h_i to be at least $O(\delta_t)$:

$$h_i=\delta_t h_i^{(1)}+\delta_t^2 h_i^{(2)}+\delta_t^3 h_i^{(3)}+\cdots, \tag{8}$$

in which, we emphasize, there is no ''equilibrium'' $O(\delta_t^0)$ h_i term.

It is natural to take the lead term $\delta_t h_i^{(1)}$ to be zeroth order in velocity gradients (this ensures consistency with several previous LB applications in which the lattice fluid is body forced by a spatially uniform pressure gradient; see, e.g., [15] and the references therein). Accordingly we take $h_i^{(1)}$ to be zeroth order in gradient quantities, and $h_i^{(2)}$ to contain any first order gradients in macroscopic observables $\rho,\mathbf{v}$; that is, in general $h_i^{(n)}$ contains $(n-1)$th order gradients in ρ and $\mathbf{v}$.

The question now is to determine the $h_i^{(n)}$ that give Eqs. (5) and (6) in a consistent fashion. From a Chapman-Enskog type expansion of the Taylor expanded evolution equation (7), after Hou *et al.* [14], we obtain at $O(\delta_t)$

$$(\partial_{t0}+c_{i\gamma}\partial_\gamma)f_i^{(0)}=-\frac{1}{\tau}f_i^{(1)}+h_i^{(1)}, \tag{9}$$

and at $O(\delta_t^2)$

$$\partial_{t1}f_i^{(0)}+(\partial_{t0}+c_{i\gamma}\partial_\gamma)\left(1-\frac{1}{2\tau}\right)f_i^{(1)}=-\frac{1}{\tau}f_i^{(2)}+h_i^{(2)}. \tag{10}$$

It is usual, in deriving the macroscopic dynamics, to substitute for $f_i^{(1)}$ in Eq. (10), using Eq. (9). We then have

$$\partial_{t1}f_i^{(0)}+(\partial_{t0}+c_{i\gamma}\partial_\gamma)\left(1-\frac{1}{2\tau}\right)[-\tau(\partial_{t0}+c_{i\delta}\partial_\delta)f_i^{(0)}+\tau h_i^{(1)}]$$

$$=-\frac{1}{\tau}f_i^{(2)}+h_i^{(2)}. \tag{11}$$

We do not use Eqs. (9)–(11) to relate $f_i^{(n)}$ to the $h_i^{(n)}$. Rather, we now choose to partition the problem in such a way as to recover the RHS (LHS) terms in the target equations (5) and (6) from the $h_i^{(n)}$ ($f_i^{(n)}$) independently.

Writing $\Delta_{i\alpha}$ for $c_{i\alpha}$ or 1, we take moments of Eqs. (9) and (11) and for the $f_i^{(n)}$ set

$$\partial_{t0}\sum_i f_i^{(0)}(\mathbf{v},\rho)\Delta_{i\alpha}+C_{i\gamma}\partial_\gamma\sum_i f_i^{(0)}(\mathbf{v},\rho)\Delta_{i\alpha}=$$

$$-\frac{1}{\tau}\sum_i f_i^{(1)}\Delta_{i\alpha}, \tag{12}$$

$$\sum_i\left[\partial_{t1}+\left(\frac{1}{2}-\tau\right)(\partial_{t0}+c_{i\gamma}\partial_\gamma)^2\right]f_i^{(0)}(\mathbf{v},\rho)\Delta_{i\alpha}$$

$$=-\frac{1}{\tau}\sum_i f_i^{(2)}\Delta_{i\alpha}, \tag{13}$$

where

$$\Delta_{i\alpha}=c_{i\alpha},1. \tag{14}$$

This, taken with the usual constraints

$$\sum_i f_i^{(0)}(\mathbf{v},\rho)=\rho,$$

$$\sum_i f_i^{(0)}(\mathbf{v},\rho)c_{i\alpha}=\rho v_\alpha, \tag{15}$$

$$\sum_i f_i^{(0)}(\mathbf{v},\rho)c_{i\alpha}c_{i\beta}=\rho\delta_{\alpha\beta}/c_s^2+\rho v_\alpha v_\beta,$$

corresponds to the unadjusted isothermal LBGK scheme [10,13], which we use without further modification to recover the LHS terms in the model's macrodynamics [Eqs. (5) and (6)].

Implicitly, therefore, the corresponding moments of the h_i,

$$\sum_i h_i^{(1)}\Delta_{i\alpha}, \tag{16}$$

$$\tau\left(1-\frac{1}{2\tau}\right)\sum_i (\partial_{t0}+c_{i\gamma}\partial_\gamma)h_i^{(1)}\Delta_{i\alpha}-\sum_i h_i^{(2)}\Delta_{i\alpha}, \tag{17}$$

must be used to insert the new terms [the RHS's of Eqs. (5) and (6) here]. Note that the expressions (16) and (17) operate at $O(\delta_t)$ and $O(\delta_t^2)$, respectively.

Moments (16) and (17) can now be used to insert target terms into the lattice continuity and momentum equations—for present purposes, the terms in the RHS's of Eqs. (5) and (6). Care must be exercised; as is evident from expressions (16) and (17), the choice of $h_i^{(1)}$ must influence the form of $h_i^{(2)}$ and so forth.

For our particular application (of pipe flow) we shall first select a form for the $h_i^{(1)}$ that yields the desired modification of the lattice continuity equation (5). Thereafter the $h_i^{(2)}$ will be determined from the chosen $h_i^{(1)}$ and the target modification to the lattice fluid's momentum equations.

B. Lattice continuity equation and $h_i^{(1)}$

We proceed to consider the modifications to the lattice continuity equation resulting from the inclusion of forcing terms $h_i^{(1)}$ and $h_i^{(2)}$ into the lattice evolution equation. Summing on i in Eq. (9) we obtain at $O(\delta_t)$

$$\partial_{t0}\rho+\partial_\beta\rho v_\beta=\sum_i h_i^{(1)}, \tag{18}$$

which, with the target dynamics [of Eqs. (5) and (6)] in view, motivates the following selection of $h_i^{(1)}$:

$$h_i^{(1)}\equiv t_p\left(\mathcal{G}c_{ix}-\frac{\rho v_y}{y}\right), \tag{19}$$

where $\mathcal{G}$ is a position and time independent parameter for the forcing magnitude and $t_p=1/9$ for i with $|\mathbf{c}_i|=1$, 1/36 for i with $|\mathbf{c}_i|=\sqrt{2}$, and 4/9 for $i=0$ [13,14]. With this choice the RHS of Eq. (18) takes the desired form:

$$\sum_i h_i^{(1)}=\sum_i t_p\left(\mathcal{G}c_{ix}-\frac{\rho v_y}{y}\right)$$

$$=\mathcal{G}\sum_i t_p c_{ix}-\frac{\rho v_y}{y}\sum_i t_p=-\frac{\rho v_y}{y}. \tag{20}$$

We proceed to $\mathcal{O}(\delta_t^2)$ now. Summing on i in Eq. (11) we obtain, in the LHS of the lattice continuity equation, the additional expression

$$\tau\left(1-\frac{1}{2\tau}\right)\left[\partial_{t0}\sum_i h_i^{(1)}+\partial_\gamma\sum_i h_i^{(1)}c_{i\gamma}\right]-\sum_i h_i^{(2)}, \tag{21}$$

which, with our target dynamics in view, should vanish. Using Eqs. (19) and (20) therefore

$$\sum_i h_i^{(2)}=\left(\tau-\frac{1}{2}\right)\left[\partial_{t0}\sum_i t_p\left(\mathcal{G}c_{ix}-\frac{\rho v_y}{y}\right)\right.$$

$$\left.+\partial_\gamma\sum_i t_p\left(\mathcal{G}c_{ix}-\frac{\rho v_y}{y}\right)c_{i\gamma}\right], \tag{22}$$

which, since $\mathcal{G}$ is constant in space and time, becomes

$$\sum_i h_i^{(2)}=\left(\tau-\frac{1}{2}\right)\left[\partial_{t0}\sum_i\left(-t_p\frac{\rho v_y}{y}\right)+0\right]. \tag{23}$$

Hence we have a condition on the $h_i^{(2)}$,

$$\sum_i h_i^{(2)}=\left(\frac{1}{2}-\tau\right)\frac{1}{y}\partial_{t0}\rho v_y, \tag{24}$$

further consideration of which is postponed to the next section.

C. Lattice momentum equation and $h_i^{(2)}$

With an appropriately modified continuity equation secured, we proceed to consider the lattice Euler equation, which should gain a term, at $O(\delta_t)$, by our choice of $h_i^{(1)}$ [Eq. (19)]. To see this, multiply Eq. (11) by $\mathbf{c}_i$ and sum on i to obtain

$$\partial_{t0}\rho v_\alpha+\partial_\beta\Pi_{\alpha\beta}^{(0)}=\sum_i h_i^{(1)}c_{i\alpha}$$

$$=\sum_i \mathcal{G}c_{ix}c_{i\alpha}-\frac{\rho v_y}{y}\sum_i t_p c_{i\alpha}$$

$$=\frac{1}{3}\mathcal{G}\delta_{\alpha x}, \tag{25}$$

where we have used the result $\Sigma_i t_p c_{i\alpha}c_{i\beta}=\delta_{\alpha\beta}/3$ [14] for a 2D9Q lattice. Clearly, the lattice fluid's Euler equation gains a body force density term which is widely used to mimic the effect of a *spatially uniform* body force (pressure gradient) impressed throughout the lattice fluid:

$$\partial_{t0}\rho v_y=-\partial_\beta\Pi_{y\beta}^{(0)}. \tag{26}$$

But the equilibrium momentum flux tensor

$$\Pi_{\alpha\beta}^{(0)}\equiv-\frac{1}{3}\rho\delta_{\alpha\beta}+\rho v_\alpha v_\beta \tag{27}$$

still contains pressure gradient terms $\rho\delta_{\alpha\beta}/3$, we emphasize. Using Eq. (26) we can recast condition (24) as

$$\sum_i h_i^{(2)} = \left(\frac{1}{2} - \tau\right)\frac{1}{y}\partial_{t0}\rho v_y = -\left(\frac{1}{2} - \tau\right)\frac{1}{y}\partial_\beta \Pi_{y\beta}^{(0)} \quad (28)$$

and substituting for $\Pi_{\alpha\beta}^{(0)}$ this becomes

$$\sum_i h_i^{(2)} = \left(\tau - \frac{1}{2}\right)\frac{1}{y}\partial_\beta\left(-\frac{1}{3}\rho\delta_{y\beta} + \rho v_\beta v_y\right)$$

$$= \left(\tau - \frac{1}{2}\right)\frac{1}{y}\left[-\frac{1}{3}\partial_y\rho + \partial_\beta\rho v_\beta v_y\right]. \quad (29)$$

At $O(\delta_t^2)$ now, multiply Eq. (11) by $\mathbf{c}_i$ and sum on i to obtain the additional terms generated by our forcing in the LHS of the lattice Navier-Stokes equation:

$$\tau\left(1 - \frac{1}{2\tau}\right)\left[\partial_{t0}\sum_i h_i^{(1)}c_{i\alpha} + \partial_\gamma\sum_i h_i^{(1)}c_{i\alpha}c_{i\gamma}\right] - \sum_i h_i^{(2)}c_{i\alpha}$$

$$= \tau\left(1 - \frac{1}{2\tau}\right)\left[0 + \partial_\gamma\left(-\frac{\rho v_y}{y}\right)\sum_i t_p c_{i\alpha}c_{i\gamma}\right] - \sum_i h_i^{(2)}c_{i\alpha}$$

$$= \frac{1}{3}\left(\tau - \frac{1}{2}\right)\partial_\alpha\left(-\frac{\rho v_y}{y}\right) - \sum_i h_i^{(2)}c_{i\alpha}$$

$$= \nu(\tau)\partial_\alpha\left(-\frac{\rho v_y}{y}\right) - \sum_i h_i^{(2)}c_{i\alpha}, \quad (30)$$

where we have used the fact that $\partial_{t0}\Sigma_i h_i^{(1)}c_{i\alpha} = \partial_{t0}(\mathcal{G}\delta_{\alpha x}/3) = 0$, and $\nu(\tau)$ denotes the kinematic viscosity of the lattice fluid [13]. Expression (30) is required to supply additional target terms to match those in the RHS of the Navier-Stokes equation (6). Hence we write

$$-\left[\nu\partial_\alpha\left(-\frac{\rho v_y}{y}\right) - \sum_i h_i^{(2)}c_{i\alpha}\right] = \frac{\nu}{y}\left(\partial_y v_\alpha - \frac{1}{y}v_y\delta_{\alpha y}\right) \quad (31)$$

and, rearranging,

$$\sum_i h_i^{(2)}c_{i\alpha} = \nu\left[\frac{1}{y}\partial_y\rho v_\alpha - \frac{1}{y^2}\delta_{\alpha y}\rho v_y + \partial_\alpha\left(-\frac{\rho v_y}{y}\right)\right]$$

$$= \frac{\nu}{y}[\partial_y\rho v_\alpha - \partial_\alpha\rho v_y] \quad (32)$$

by the product rule.

From Eqs. (29) and (32) we have expressions for the moments of the $h_i^{(2)}$ as follows:

$$\sum_i h_i^{(2)} = \frac{3\nu}{y}\left[-\frac{1}{3}\partial_y\rho + \partial_\beta\rho v_\beta v_y\right], \quad (33)$$

$$\sum_i h_i^{(2)}c_{i\alpha} = \frac{\nu}{y}[\partial_y\rho v_\alpha - \partial_\alpha\rho v_y], \quad (34)$$

where, note, the RHS of the latter is equivalent to $\nabla\times(\rho\mathbf{v})|_z^\wedge$.

By inspection, one choice of the $O(\delta_t^2)$ forcing term is

$$h_i^{(2)} = 3t_p\frac{\nu}{y}\delta_t^2\left[\left(-\frac{1}{3}\partial_y\rho + \partial_\beta\rho v_\beta v_y\right) + (\partial_y\rho v_\beta - \partial_\beta\rho v_y)c_{i\beta}\right]. \quad (35)$$

In summary, to recover lattice fluid macrodynamics equivalent to pipe flow, while using a regular square lattice under a uniform applied pressure gradient, we require our forcing terms [Eq. (8)] to be of the form

$$h_i^{(1)} = t_p\left(\mathcal{G}c_{ix} - \frac{\rho v_y}{y}\right),$$

$$h_i^{(2)} = t_p\frac{3\nu}{y}[-\partial_y\rho/3 + \partial_x\rho v_x v_y + \partial_y\rho v_y v_y + \partial_y\rho v_x c_{ix} - \partial_x\rho v_y c_{ix}]. \quad (36)$$

For purposes of performing the simulations described in the next section, the gradient terms in Eqs. (36) were evaluated using discrete difference approximations evaluated on lattice, using second order accurate expressions. However, note that stresses and higher order fluxes such as appear in (36) can be computed, more in the spirit of the lattice Boltzmann method, from appropriate higher order moments of f_i, without recourse to such finite differences, thereby avoiding the problems of instability, dissipation, and numerical inefficiency that finite difference schemes introduce.

Before we proceed to consider the implementation of the scheme embodied in Eqs. (36) some general remarks are in order.

D. Discussion

In the preceding sections we have shown how different source terms inserted into the evolution equation can be used to adjust the final form of the lattice fluid's macrodynamics. At first sight it may seem that a forcing strategy that offers $2Q$ parameters $h_i^{(n)}$, $i=1,\ldots,Q$, $n=1,2$, is flexible. However, one should sound a cautionary note. The strategy derived in Secs. III B and III C is one example of the general considerations outlined in Sec. III A. It is, moreover, somewhat sanitized. For, in our example, the $h_i^{(1)}$'s and $h_i^{(2)}$'s in expressions (16) and (17) may be determined independently, and in a natural manner—the form of $h_i^{(1)}$ suggests itself and therefore it can be used explicitly to determine an appropriate form for $h_i^{(2)}$. This may not be the case for other applications and it may well be that, for other problems requiring more complicated source terms, constraints arise between the $h_i^{(n)}$, effectively reducing the number of independent $h_i^{(n)}$'s available.

Clearly the particular forcing terms derived in Secs. III B and III C, against the example of pipe flow, contain gradient quantities. It may well be argued that explicit inclusion of gradients in this way is contrary to the philosophy of the lattice Boltzmann method, in that it undermines the distinction between lattice Boltzmann flow calculations and conventional finite difference Navier-Stokes solvers. However,

derivative lattice Boltzmann simulations already in the literature rely upon forcing with gradient quantities to recover their target dynamics. Indeed, the philosophy of our approach in Sec. III reflects the fact that forcing can be applied as a practical tool, adjusting the form of the macrodynamical equations of a lattice Boltzmann fluid, which is primarily of the form of the Navier-Stokes equation. So, for such lattice Boltzmann schemes as do rely upon gradient-forced macrodynamics, the way in which we incorporate the necessary gradients quantities, through the Chapman-Enskog expansion, is, we hope, pertinent.

The strategy described in this work is envisaged as a resource for adjusting the dynamics of a *monophasic* lattice fluid. While it can, in principle, modify the dynamics of a lattice Boltzmann scheme whatever the physical origin of the additional terms in the momentum/continuity equations [RHS's of Eqs. (5) and (6)], our approach here still incorporates such terms carefully but phenomenologically. In particular, this work does not have the same fundamental basis in the full Boltzmann equation as the forcing strategies that have very recently appeared [12]. The work reported in Ref. [12] formally addresses external acceleration terms $\boldsymbol{a}\cdot\boldsymbol{\nabla}_{\xi}f_i$ in the LHS of a generalized Boltzmann equation and adopts a satisfying *a priori* approach to the problem of forcing lattice fluid flow. Probably it would be contrary to the philosophy of the work, but the analysis of Ref. [12] can obtain the effective forcing for our present problem of cylindrical pipe flow as follows.

In the notation [12], those corrections to the lattice continuity (momentum) equation in the RHS of Eq. (5) are obtained by generalizing constraint equations 12(a) and 12(b) of Ref. [12] to

$$\int d\boldsymbol{\xi}\mathbf{a}\cdot\boldsymbol{\nabla}_{\xi}f=F_0, \tag{37}$$

$$\int d\boldsymbol{\xi}\boldsymbol{\xi}\mathbf{a}\cdot\boldsymbol{\nabla}_{\xi}f=F_1 \tag{38}$$

with

$$F_0=-\frac{1}{y}\rho v_y,$$

$$F_{1\alpha}=-\frac{\nu}{y}\partial_y\rho v_{\alpha}-\frac{\nu\rho v_y}{y^2}\delta_{\alpha y}. \tag{39}$$

Following Ref. [12], the integrations in Eqs. (37) and (38) work through a formal discretization of the Boltzmann equation to generate summations in the emergent LBGK scheme, expressing the presence of forcing (strictly, for present purposes, an *effective* forcing) given by

$$\mathbf{a}\cdot\boldsymbol{\nabla}_{\xi}f\rho t_p(c^{(0)}+c_i^{(1)}\xi_i+c_{ij}^{(2)}\xi_i\xi_j+\cdots). \tag{40}$$

The coefficients $c^{(n)}$ depend on hydrodynamic variables and their gradients. By substituting the truncated series expansion of $\mathbf{a}\cdot\boldsymbol{\nabla}_{\xi}f$ into the constraints of Eqs. (37) and (38), one can obtain the coefficients $c^{(n)}$ up to a certain order in $\mathbf{u}$ consistent with the Chapman-Enskog analysis. It can be shown that the above analysis leads to the same results as we obtain here.

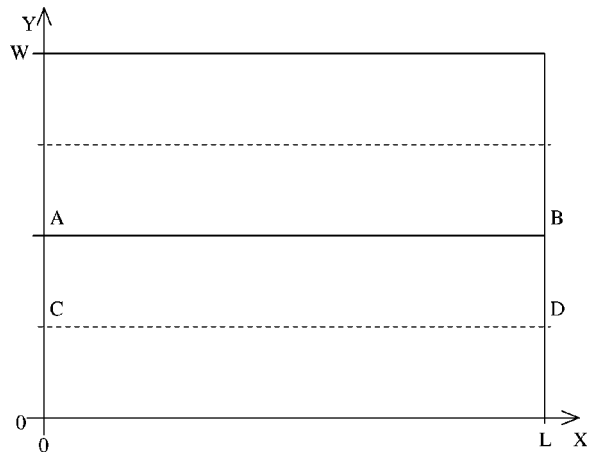

FIG. 1. Schematic of our test-bench implementation of uniform pipe flow. Below (above) line *AB* the lattice fluid is body forced toward the right (left). Duct axes (broken lines) should be located off lattice, which can be achieved by appropriate positioning of the periodic boundaries that obtain between left and right and between top and bottom of the lattice.

IV. SIMULATION OF PIPE FLOW

In this section we discuss results from a test-bench simulation of forced flow in an infinitely long circular pipe, driven by a uniform pressure gradient (effective body force density) parallel with the pipe axis. Figure 1 is a schematic of our implementation. We shall represent the discrete lattice coordinates with integers X and Y; in this figure, X represents the distance along the pipe in the direction of flow. All the results reported relate to a steady-state lattice initialized with node density $\rho=1.0$. Convergence was checked by monitoring the time development of the lattice velocity field residuals.

Periodic boundaries were installed along vertical lines $X=0$ and $X=L$. We shall return to the issue of horizontal boundaries shortly. Flow was forced (see below) parallel to the X direction. Thus the overall algorithm is translationally invariant along the horizontal. Under such circumstances it is possible to make the lattice length L conveniently small and also to avoid any axial lattice fluid density gradient, which might otherwise lead to compressibility error [16].

Consider the half of the simulation below the horizontal line connecting *A* and *B*. Here fluid was induced to flow in the direction from *A* to *B* by use of a positive body force constant $\mathcal{G}$, corresponding to an applied pressure gradient of $\mathcal{G}/3$, $\mathcal{G}>0$ [Eq. (26)]. For this region of the lattice the pipe axis is the broken line connecting *C* with *D*, which corresponds to $y=0$. Since certain of the forcing terms in Eqs. (35) and (36) refer to the reciprocal of y (distance from the pipe axis), care must be exercised to avoid any singularity. Accordingly the line *CD* should be located off lattice, which can be achieved by appropriate positioning of the horizontal no-slip lattice boundaries.

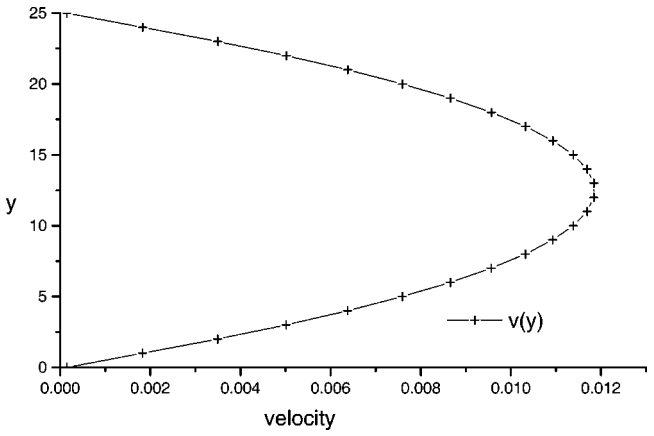

FIG. 2. Variation of axial velocity $v_x(Y)$ with position Y in the lower half of the simulation lattice (below line AB, Fig. 1). As a result of the particular forcing strategy employed the resulting flow profile is exactly parabolic with on-lattice zeros of velocity in the lines $Y=0$ and $Y=W/2$.

The general problem of terminating an LB lattice so as to impose a no-slip condition on the lattice fluid velocity field is unsolved. However, a number of methods that closely mimic the effect of friction on the flow have been devised; for a discussion, see [16] and references therein. The symmetry of our particular problem can be exploited, however. In fact periodic boundary conditions were also applied, along the lines $Y=0$ and $Y=W$, with the upper layer of lattice fluid (above the line connecting A with B) forced back by use of a negative body force constant $-\mathcal{G}$ [Eq. (26)] for $Y>W/2$, which, of course, has the effect of forcing this top fluid layer toward the left. Where our two lattice fluids contact, in the lines $Y=0$ (equivalent to the periodic image line $Y=W+1$) and $Y=W/2$, a zero of velocity (no-slip boundary) must, on general grounds, occur. Two opposing parabolic flow profiles were thus established for a range of LBGK collision parameter (lattice fluid kinematic viscosity) values.

Figure 2 shows the variation of axial velocity v_x with position Y in the lower half of the simulation lattice (below line AB, Fig. 1). As a result of the particular flow forcing strategy and lattice closure the resulting flow profile is exactly parabolic with on-lattice zeros of velocity in the lines $Y=0$ and $Y=W/2$.

The Darcy-Weisbach friction factor, defined through the usual relationship

$$\frac{dP}{dz}=f\frac{1}{H_d}\frac{1}{2}\rho V^2, \tag{41}$$

where H_d is the hydraulic diameter (the physical diameter d for a circular pipe) and V the average velocity (half the peak velocity), was measured over the full range of LBGK collision parameter $1/\tau$. Figure 3 shows f expressed as a ratio with F, the analytical value for a fully developed, laminar, pipe flow:

$$F=\frac{64}{\mathrm{Re}},\quad \mathrm{Re}=\frac{d\,V}{\nu}. \tag{42}$$

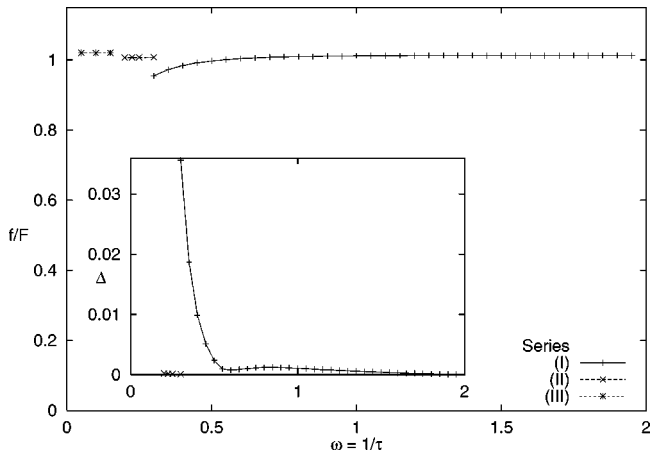

FIG. 3. Measured value of Darcy-Weisbach friction factor expressed as a ratio with the analytic value. The data presented here are for constant Reynolds number $\mathrm{Re}=10$. The discontinuity in the region of $1/\tau=0.3$ demonstrates the effect of an increase in spatial resolution between series (I) ($+$ points, $W=50$) and series (II) ($\times$ points, $W=302$). The inset shows variation of simulation error Δ over the same range of $1/\tau$ as for series (I) and (II).

The data presented in Fig. 3 correspond to a Reynolds number $\mathrm{Re}=10$, which was kept constant by varying the simulation pressure gradient parameter $\mathcal{G}$ in accordance with the relationship

$$\mathcal{G}=\frac{64}{3}\,\mathrm{Re}\,\frac{\rho(2-\omega)^2}{W^3\omega^2} \tag{43}$$

derived for pipe flow [11], using Eq. (25) and the fact that our simulated pipe radius is $W/4$ (Fig. 1). In effect, the lattice width W not only determines the effective pipe diameter, for constant Re it also determines the spatial resolution of the simulation.

The data presented in Fig. 3 are in three series: (I) for $0.3\leqslant 1/\tau<2.0$, $W=50$ ($+$ points), (II) for $0.2\leqslant 1/\tau\leqslant 0.3$ with substantially increased spatial resolution, $W=302$ ($\times$ points), and (III) $0.0<1/\tau\leqslant 0.15$, $W=102$ (* points). The measured departure from the analytic steady-state pipe flow profile, $V_x(\mathbf{r})$,

$$\Delta=\sum_{\mathbf{r}}\,|V_x(\mathbf{r})-v_x(\mathbf{r})|, \tag{44}$$

varies as $3\times10^{-5}<\Delta<3.5\times10^{-2}$ over the data series (I). These data are presented in the inset to Fig. 3 over the same range of $1/\tau$ covered by series (I) and (II). However, it is clear from Fig. 3 that this increase in error as $1/\tau$ approaches the (arbitrary) value of 0.3, in series (I), can be combated by increasing the spatial resolution (value of W), as for series (II). So the accuracy of the numerical calculation (in terms of the velocity field) can be maintained at second order, even for small values of $1/\tau$, given sufficient spatial resolution. Below the value $1/\tau\approx0.2$, an observed instability associated with the singularity of y [Eqs. (36)] means that the spatial resolution necessary for convergence greatly increases, and the data shown in series (III) of Fig. 3, for values of $1/\tau$

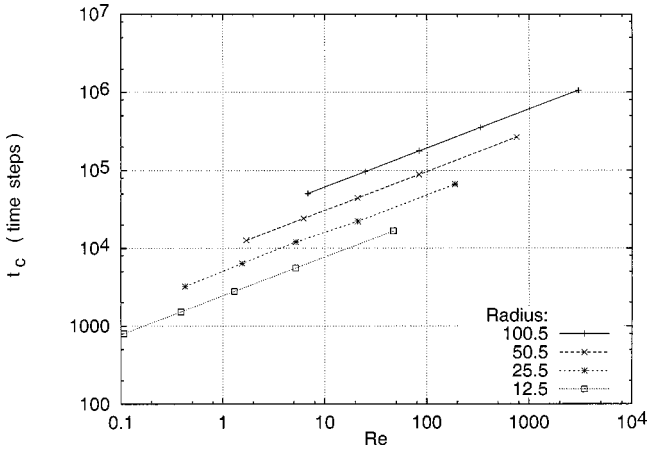

FIG. 4. Convergence time data for four lattice sizes corresponding to channels of width $W/2=25$, 51, 101, and 201 over a range of relaxation parameter $0.6\leqslant 1/\tau\leqslant 1.8$.

$\leqslant 0.15$, were obtained using an analytic expression for the terms in Eqs. (36) in our code. Note also that the convergence time, assessed in terms of time changes in the velocity field residual,

$$R=\sum_{\mathbf{r}} [v_x(\mathbf{r},t+1)-v_x(\mathbf{r},t)]^2, \tag{45}$$

varies substantially over the range of data represented in Fig. 3, and also with Reynolds number.

The factor $1/y$ that is attached to certain terms in our expressions (36) for $h_i^{(1)}$ and $h_i^{(2)}$ is, of course, peculiar to our chosen example problem of adjusting for cylindrical pipe flow, but its singularity clearly affects convergence behavior.

In order to assess convergence time with varying spatial resolution, data were collected over a range of Reynolds number, for channels of width $W/2=25$, 51, 101, and 201. In all cases the correct laminar flow profile and friction factor were eventually obtained in good agreement with theory. The different convergence times for these checks are summarized in Fig. 4. Note that for all the data in Fig. 4 the lattice collision parameter was confined to the range $0.6<1/\tau<1.85$.

Figure 5 shows the convergence behavior of the scheme in terms of the error [defined in Eq. (44)] as a function of spatial resolution. The Reynolds numbers used in these simulations varied over the range $1\leqslant \mathrm{Re}\leqslant 100$ and the spatial resolution (measured by the value of W, the simulation width) over a range corresponding to channel radii $12.5\leqslant R \leqslant 250.5$.

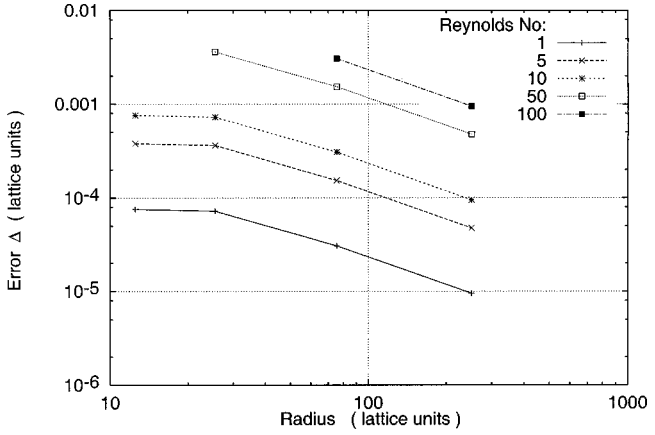

FIG. 5. Convergence behavior. Error Δ defined as departure from the analytic solution [Eq. (44)] plotted as a function of spatial resolution. For the data shown here the range of Reynolds number is $1\leqslant \mathrm{Re}\leqslant 100$. The spatial resolution is measured by the value of $R=W/4$ (channel radius in lattice units) which varies over the range 12.5 to 250.5.

V. CONCLUSION

In this work we have shown how a forcing strategy, applied to the microscopic evolution equation of a lattice Boltzmann fluid, can correctly modify the emergent macroscopic equations toward a particular target form. For purposes of deriving the model's macrodynamics (within the usual Chapman-Enskog expansion) our strategy treats any forcing terms (source terms) that are added into the microdynamical evolution equation in a manner consistent with the momentum densities. We find that forcing terms treated in this way occur, as it were, ''recursively'' in the macrodynamics [see Eqs. (16) and (17)] and in consequence their inclusion into a lattice Boltzmann scheme is somewhat more involved than one might naively imagine. For our chosen application, in which there are no constraints on the forcing problem, it is straightforward to determine a set of forcing terms systematically.

While we work here with a lattice Bhatnagar-Gross-Krook scheme and consider, for definiteness, the case of flow in a circular cross-section duct (results from a test-bench simulation are in excellent agreement with theory, note) our methodology can clearly be generalized to any lattice Boltzmann scheme. (Here we note that any constraints on the forcing problem will reduce the number of independent forcing terms.) In this respect the present work should be of interest to any worker attempting to adjust the macrodynamical equations of a lattice Boltzmann scheme for, e.g., applications in nematodynamics or viscoelasticity.

[1] U. Frisch, D. d'Humières, B. Hasslacher, P. Lallemand, Y. Pomeau, and J. P. Rivet, Complex Syst. **1**, 649 (1987).
[2] X. He and L. S. Luo, Phys. Rev. E **56**, 6811 (1997).
[3] G. R. McNamara and G. Zanetti, Phys. Rev. Lett. **61**, 2332 (1988).
[4] F. Higuera and J. Jiménez, Europhys. Lett. **9**, 663 (1989).
[5] S. Chen, H. Chen, D. Martinez, and W. H. Matthaeus, Phys. Rev. Lett. **67**, 3776 (1991).
[6] S. Chen, H. Chen, and W. H. Matthaeus, Phys. Rev. A **45**, R5339 (1992).
[7] R. Benzi, S. Succi, and M. Vergassola, Phys. Rep. **222**, 145 (1992).

[8] S. Succi, R. Benzi, and F. J. Higuera, Physica D **47**, 219 (1991).
[9] P. Bhatnagar, E. P. Gross, and M. K. Krook, Phys. Rev. **94**, 511 (1954).
[10] Q. Zou, S. Hou, S. Chen, and G. D. Doolen, J. Stat. Phys. **81**, 319 (1995).
[11] L. D. Landau and E. M. Lifschitz, *Fluid Mechanics*, 2nd ed. (Pergamon, Oxford, 1987).
[12] L. S. Luo, Phys. Rev. Lett. **81**, 1618 (1998); Phys. Rev. E **62**, 4982 (2000).
[13] Y. H. Qian, D. d'Humières, and P. Lallemand, Europhys. Lett. **17**, 479 (1992).
[14] S. Hou, Q. Zou, S. Chen, G. D. Doolen, and A. C. Cogley, J. Stat. Phys. **118**, 329 (1995).
[15] L. S. Luo, J. Stat. Phys. **88**, 913 (1997).
[16] D. M. White, I. Halliday, C. M. Care, and A. Stevens, Physica D **129**, 68 (1999).